

# Quantitative phenotype characterization of developing mouse brains by diffusion tensor imaging: Application for the Frizzled-4-/- mutant mice

M. Aggarwal<sup>1</sup>, X. Ye<sup>2</sup>, J. Nathans<sup>2,3</sup>, M. I. Miller<sup>1,4</sup>, S. Mori<sup>5</sup>, and J. Zhang<sup>5</sup>

<sup>1</sup>Department of Biomedical Engineering, Johns Hopkins University School of Medicine, Baltimore, MD, United States, <sup>2</sup>Department of Molecular Biology & Genetics, Johns Hopkins University School of Medicine, Baltimore, MD, United States, <sup>3</sup>Department of Neuroscience, Johns Hopkins University School of Medicine, Baltimore, MD, United States, <sup>4</sup>Center of Imaging Science, Johns Hopkins University, Baltimore, MD, United States, <sup>5</sup>Department of Radiology, Johns Hopkins University School of Medicine, Baltimore, MD, United States

**Introduction:** It has been shown that high resolution diffusion tensor imaging (DTI) is a powerful tool for characterizing mouse brain phenotype<sup>1</sup>. DTI can provide unique neuroanatomical information not readily available by histology, and has been used to characterize developmental abnormalities in several mutant mouse strains<sup>2</sup>. We are developing quantitative approaches that can efficiently examine phenotypic changes throughout the entire brain. In this study, we report population-based quantitative analyses of DTI datasets of developing mouse brains, applied to the Frizzled-4 knockout ( $Fz4^{-/-}$ ) mouse model. Histological analyses of the  $Fz4^{-/-}$  mouse brain have shown progressive cerebellar degeneration, with apoptosis of granule cells after the second postnatal week, followed by progressive loss of Purkinje cells through adulthood<sup>3</sup>. We used high resolution DTI to study the phenotypic changes during development in the  $Fz4^{-/-}$  mouse brain.

**Methods:** MRI of *ex vivo* perfusion-fixed brains from  $Fz4^{-/-}$  mice at postnatal day 7 (P7), P14, P21 and P30 ( $n = 3$  at each age), and age-matched wild-type (WT) control mice ( $n \geq 3$  at each age) was performed. DTI images were acquired on an 11.7T NMR spectrometer, using a diffusion weighted multiple spin echo sequence (ETL = 4, TE/TR = 28/700 ms, NA = 2, b value = 1200–1500 s/mm<sup>2</sup>, at least six diffusion directions, total scan time  $\geq 24$  h per sample). The isotropic native resolution was 75  $\mu$ m for P7, 120  $\mu$ m for P14, and 125  $\mu$ m for P21 and P30 brain images (uniform relative resolution with respect to the total cerebellar volume). The diffusion tensor was diagonalized to obtain three pairs of eigenvalues and corresponding eigenvectors. Direction encoded color (DEC) maps were computed from the primary eigenvector and fractional anisotropy (FA) images. For each voxel, the ratio between the red, green and blue components was defined by the ratio of the absolute values of x, y and z components of the primary eigenvector, and the intensity was proportional to FA. Average diffusion weighted (aDW) images were the sum of all diffusion weighted images. At each developmental age, a WT brain image was chosen as the reference. Images of  $Fz4^{-/-}$  and WT mouse brains were spatially normalized to the age matched reference image, using nonlinear two-channel large deformation diffeomorphic metric mapping (LDDMM)<sup>4</sup> based on the aDW and FA contrasts. At each developmental stage, the spatially normalized tensor data (after re-orientation) were averaged for each of the two groups (wt and  $Fz4^{-/-}$ ), and the average FA and DEC maps were computed from the average tensor data. A FA difference map was generated by computing the difference of average FA images for the WT and  $Fz4^{-/-}$  groups at each age. The difference map quantitatively captures the sample-averaged regional differences in diffusion anisotropy between age matched WT and  $Fz4^{-/-}$  mouse brains.

**Results & Discussion:** Fig. 1 shows the population-averaged mid-sagittal DEC maps of the WT and  $Fz4^{-/-}$  mouse cerebellum, at P7, P14, P21 and P30. In Fig. 1, WT mouse cerebellar cortex has relatively high FA ( $0.35 \pm 0.04$  at P30) and a distinct pattern. The red layer corresponds to the molecular layer of the cerebellar cortex, which contains massive granule cell parallel fibers running parallel to the pia surface, the green layer contains the Purkinje cell fibers, and the blue layer contains the cerebellar white matter. At P7, no significant differences could be observed between the WT and  $Fz4^{-/-}$  cerebellums. From P14 to P30, a progressive decrease in FA as well as a reduction in the thickness of the red layer in the cerebellar cortex was observed in the  $Fz4^{-/-}$  mice, as compared to age matched WT controls. At P30, the average DEC map of the  $Fz4^{-/-}$  cerebellum was marked by reduced FA and an almost complete absence of the red layer in the cerebellar cortex (indicated by white arrows in Fig. 1). The FA difference maps revealed regions in the developing  $Fz4^{-/-}$  brain with anomalies in FA as compared to WT brains. Fig. 2 shows coronal sections from average FA maps at P7, P14 and P30, showing semi-sections from the WT (left) and mirrored  $Fz4^{-/-}$  (right) brains in the left panel. The difference

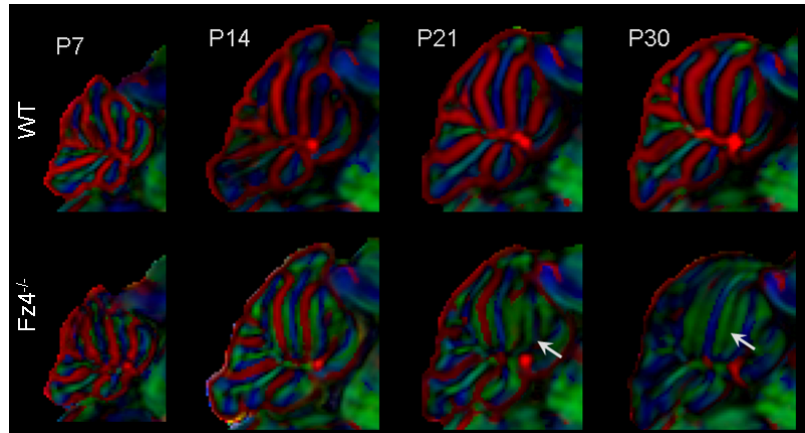


**Fig. 1:** Population averaged DEC maps of the mid-sagittal cerebellums in WT and  $Fz4^{-/-}$  brains at P7, P14, P21 and P30 reveal progressive degeneration of parallel fibers in the  $Fz4^{-/-}$  cerebellum. Red, green and blue denote fibers along the medial-lateral, rostral-caudal and dorsal-ventral axes respectively. White arrows indicate regions of low FA in the  $Fz4^{-/-}$  cerebellums.

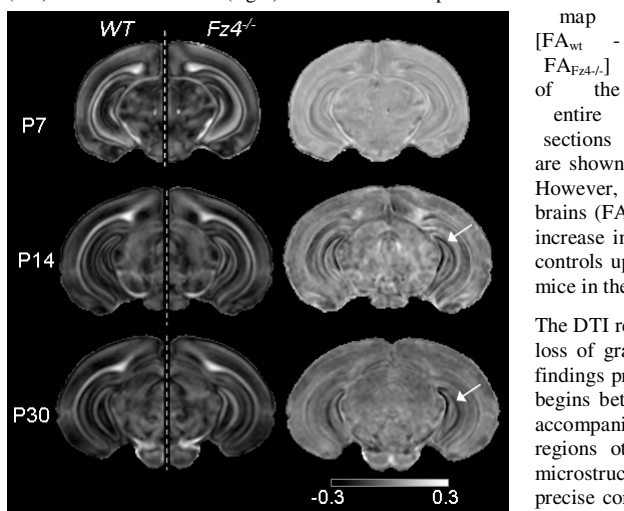


**Fig. 2:** Population-averaged FA differences in the dentate gyrus of  $Fz4^{-/-}$  and WT mouse brains. Left) Coronal semi-sections from WT (right) and  $Fz4^{-/-}$  brains at P7, P14 and P30. Right) FA difference maps ( $FA_{WT} - FA_{Fz4^{-/-}}$ ). White arrows indicate regions of higher FA in the dentate gyrus of  $Fz4^{-/-}$  brains.

are shown in the right panel. At P7, no significant differences were observed between the two groups. However, starting at P14, the  $Fz4^{-/-}$  brains showed increased FA in the dentate gyrus compared to WT brains (FA increase of  $0.16 \pm 0.04$  and  $0.17 \pm 0.05$  for the P14 and P30 age groups respectively). This increase in FA was observed consistently in all individual  $Fz4^{-/-}$  brains compared to their age-matched controls upto the fourth postnatal week. In addition, the mean FA was consistently lowered in the  $Fz4^{-/-}$  mice in the olfactory bulb, the optic tract and the fasciculus retroflexus compared to WT controls.

The DTI results suggest a progressive disorganization of the cerebellar structure and a temporal pattern of loss of granule cell parallel fibers in the developing  $Fz4^{-/-}$  cerebellum, consistent with the histological findings previously reported. Wang *et al.* have reported apoptosis of granule cells in the  $Fz4^{-/-}$  cerebellum begins between P14 and P19<sup>3</sup>. In our study, at P14 DTI revealed a marked thinning of the red layer accompanied by a decrease in FA starting at P14 (Fig. 1). While no apparent abnormality was reported in regions other than the cerebellum in the  $Fz4^{-/-}$  brain previously, our DTI results show potential microstructural changes in several forebrain regions. While the significance of these changes and the precise correlations between structural phenotype and DTI signals remain to be investigated, our results show that high resolution DTI can be valuable for quantitative characterization of developmental changes in mutant mouse brains.

**References:** [1] Mori *et al*, *Mag Res Med* 46, 2001 [2] Andrews *et al*, *Development* 133, 2006. [3] Wang *et al*, *J Neurosci* 21, 2001. [4] Miller *et al*, *Ann Rev Biomed Eng* 4, 2002.